Final state effects in photoemission of the 4f levels of terbium and dysprosium

1990 J. Phys.: Condens. Matter 2 8801

(http://iopscience.iop.org/0953-8984/2/44/009)

J. Phys.: Condens. Matter 2 (1990) 8801–8812. Printed in the UK

Final state effects in photoemission of the 4f levels of terbium and dysprosium

P A Dowben†, D LaGraffe†, Dongqi Li†, L Dottl‡, C Hwang‡, Y Ufuktepe‡ and M Onellion‡

† Department of Physics, Syracuse University, Syracuse, NY 13244-1130, USA

‡ Department of Physics, University of Wisconsin, Madison, WI 53706, USA

Received 12 June 1990

Abstract. Many electron excitations in photoemission are observed to occur at selected photon energies leading to resonant photoemission enhancements of the 4f multiplet levels of terbium and dysprosium. We find that final state symmetry effects can alter the photon energy of the photoemission resonances of the 4f levels creating a slightly different photon energy dependence for the various 4f multiplets. Additional complications are observed because of unresolved multiplets resulting from inter-atomic correlation effects. It is final state 5d–4f interactions that give rise to a variety of valence band 4f multiplets not predicted by one-electron theory.

1. Introduction

The rare earth multiplet features have historically been an area of considerable interest and 4f resonant photoemission effects at the 5p and 4d thresholds are well established [1–5]. Recent work has suggested that there are strong final state 5d–4f interactions that occur in the photoemission process [6] resulting in pronounced satellite features. Because of the wide variety of final state configurations, intensity variations between the various multiplets are expected to reflect orbital interactions between the d and f valence bands.

Our understanding of the 4f multiplets is based upon several assumptions. Perhaps the most serious assumption that is often made is that correlation (or configuration interaction) effects in the initial and final states can be neglected [7]. P S Bagus has shown that such correlation effects will be most important when a hole is created in a shell having the same principal quantum number as an open valence orbital [8]. Such a situation arises in the resonant photoemission processes that involve a super Coster–Kronig decay. Consequently, excited state multiplet lines are observed with the 4d to 4f resonant photoemission process as a result of the wide variety of final states accessible in the many electron excitation [2]. Clearly different final states, such as the different 4f multiplets, can be influenced by restrictions upon the ion final state and the coupling between the 4f levels and unpaired 5d electrons. This is why the 4f multiplet features do not share identical partial cross-sections.

For many of the early rare earth metals, there are observed 4f satellite features not explained by simple multiplet theory [7]. These 4f satellite features are rationalized to

0953-8984/90/448801 + 12 $03.50

be a result of different screening channels [9–13]. Additional difficulties in understanding the heavy rare earth metals, with their complicated multiplet structures, may also be anticipated because the relative 4f intensities are not accurately predicted by simple multiplet theories and fractional parentage schemes [7]. The 5d valence band contributions to the multiplet final states must be considered. Terbium with a singlet $^8S_{7/2}$ feature, and dysprosium, with closely spaced $^7F_5$ and $^7F_6$ multiplets, near the Fermi energy are suitable for investigating different screening channels in photoemission from the 4f multiplets of the heavy rare earth metals.

In order to study complications contributing to the 4f rare earth metal multiplet structures, it is advantageous to study rare earth metals that do not exhibit multiple valencies. Energetic arguments [14, 15] applied to the 4f level binding energies indicate that Gd, Tb, Dy as well as Ce [9, 10] are unlikely to exhibit mixed valencies even for the different local geometries of the surface and the bulk.

2. Experimental details

The experiments were carried out in an angle resolved photoemission system described in detail elsewhere [4]. The light source for these experiments was the 800 MeV synchrotron at the Synchrotron Radiation Center dispersed by a variety of monochromators including a 6 m toroidal grating monochromator (TGM), a 3 m TGM and an extended range grasshopper (ERG). The methods for preparing clean rare earth films have been previously described [4, 6]. All photoemission results were taken with the incident light 35° to 70° off normal so that the vector potential of the incident light contains components both parallel and normal to the thin film (s and p polarizations respectively), while the photoelectrons were collected normal to the surface.

The rare earth films were studied on a wide variety of substrates including Ni(111), Cu(100), Si(111), and on FCC iron thin films deposited on Cu(100). Typically several different rare earth film thicknesses were characterized on each substrate with the thickness determined by a quartz crystal oscillator. The stated values for the film thicknesses may err substantially and must be taken only as a nominal thickness. The films are generally not ordered, as determined by low energy electron diffraction but the films were not annealed to remove disorder so as to avoid complications resulting with interdiffusion with the substrate. All films were deposited at a deposition rate of approximately 1 Å min^{-1} or less onto the substrate placed at room temperature. During the evaporations, the base pressure of the system did not exceed 5×10^{-10} Torr.

The relative 4f partial cross-sections for estimating the fractional 4f contributions were determined from photoemission spectra taken at each specific photon energy. The relative contribution of each group of multiplet 4f states was obtained from these energy distribution curves by subtraction of the background photoemission signal (using a polynomial background) and integrating the areas of the various features following deconvolution. The constant initial state (CIS) derived partial cross-sections are estimated from the peak intensities with the monochromator operating at a seriously degraded resolution and are normalized for incident photon flux using a gold diode, as has been gone in other studies [4]. Because of the degraded resolution, used to obtain a better estimate of the relative partial cross-section, these constant initial state spectra may include contributions from several multiplet features as will be indicated in the text.

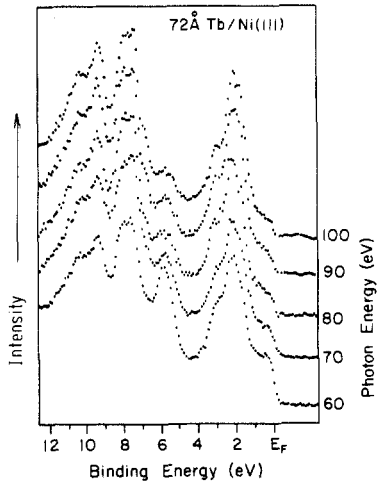

Figure 1. Photoemission spectra for a thick terbium film on Ni(111) (72 Å thick). The light incidence angle is 60° off normal and all photoelectrons were collected normal to the surface.

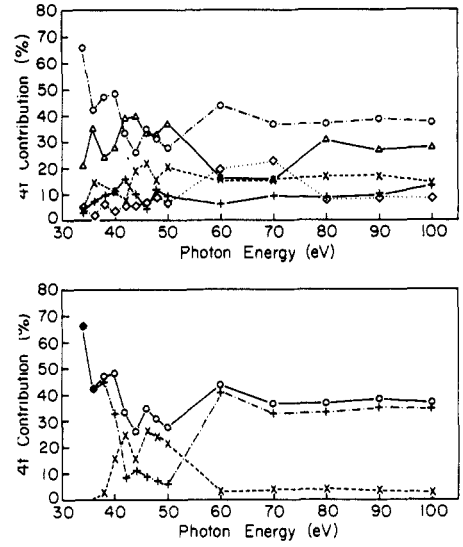

Figure 2. The relative 4f intensities for the terbium multiplet levels as a function of photon energy. The relative intensities are calculated from integral peak areas from energy distribution curves taken at each photon energy. The relative intensities are plotted (top) for the ^6F, ^6H levels (---×---); ^6G level (---+---); ^6D level (---△---); ^6I, ^6P levels (---◇---); and $^8S^{u+s}_{7/2}$ levels (---○---). The $^8S_{7/2}$ levels are shown in detail (bottom): $^8S^{u\times s}_{7/2}$ (---○---), $^8S^{u}_{7/2}$ (---×---), $^8S^{s}_{7/2}$ (---+---).

Throughout this paper, the nomenclature used to assign the 4f multiplets will denote the 4f final state ignoring the 5d contributions as is current custom in the literature.

3. Results

Following deposition of terbium on Ni(111), photoemission spectra were taken at a variety of photon energies as seen in figure 1. There is a wealth of terbium valence band features in part a result of the different 4f multiplets [16–18]. These 4f final states can be identified by comparison with x-ray photoemission spectra. The various multiplets can be found at 2.2 ± 0.1 eV ($^8S_{7/2}$), 7.6 ± 0.1 eV (^6I, ^6P), 8.0 ± 0.1 eV (^6D), 9.5 ± 0.1 eV (^6G) and 10.4 ± 0.1 (^6F, ^6H) for thick films. It should be noted that these binding energies change with coverage as has been observed for Gd overlayers [4, 19]. The $^8S_{7/2}$ multiplet exhibits two peaks, and these features will be designated as the $^8S^{u}_{7/2}$ (3.1 eV binding energy) and $^8S^{s}_{7/2}$ (2.1 eV binding energy) features, with binding energies of 3.1 ± 0.1 eV and 2.1 ± 0.1 eV respectively, at moderate coverages (two to four monolayers) and binding energies of 2.8 eV and 2.2 eV for the very thick films (more than eight monolayers).

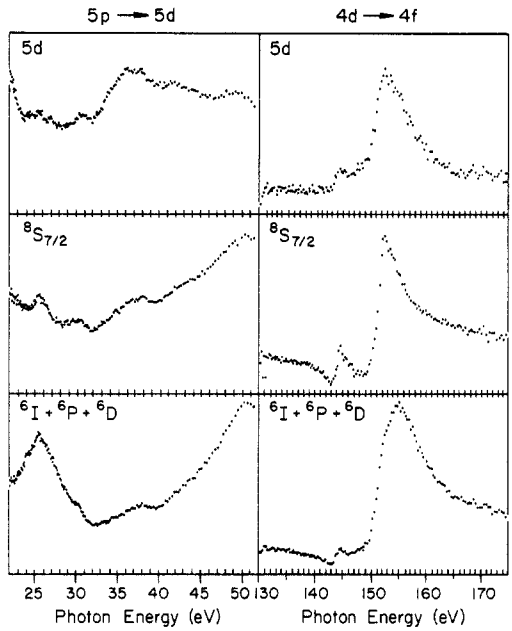

Figure 3. Constant-initial-state spectra for the terbium 5d (top), $^8S_{7/2}^{u,s}$ (middle) and $^6I + ^6P + ^6D$ (bottom) across the 5p–5d and 4d–4f resonant thresholds. Spectra were taken with an average total resolution of 0.6 eV.

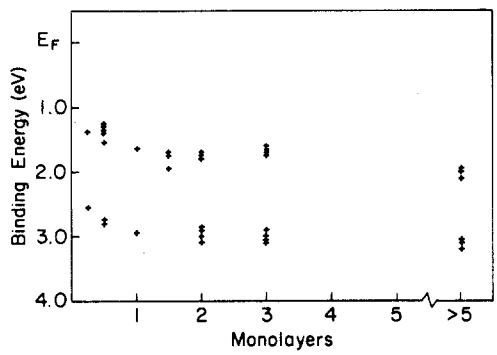

Figure 4. The binding energies of the terbium $^8S_{7/2}$ levels plotted as a function of coverage. The binding energies are references to the Fermi energy of the clean Ni(111) substrate.

While the 4f level binding energies vary little with photon energy as expected, the relative intensities vary substantially with photon energy as seen in figure 2. In general there is little resonant photoemission enhancement of the 4f multiplets, as seen in figure 3, across the 5p thresholds (28.4 ± 0.2 eV and 22.2 ± 0.2 eV) but large resonant enhancements are observed at the 4d threshold. The partial cross-sections, as determined by constant initial state spectra (shown in figure 3), clearly show that, not only do the relative 4f multiplet intensities differ with changing photon energy, but the partial cross-section of the combined $^8S_{7/2}^{u,s}$ levels differs substantially from the cross-section of the combined ^6I, ^6P and ^6D multiplet levels. In particular, the resonance at the 4d threshold (150 eV), for the $^8S_{7/2}$ occurs much more abruptly than the resonance for the combined ^6I, ^6P, ^6D feature. The $^8S_{7/2}^{u,s}$ miltiplet 4d threshold resonance occurs over a far more narrow photon energy region, i.e. 1 to 2 eV full width at half maximum, as opposed to a 4 to 6 eV full width at half maximum for the other 4f features. For the ^6I,

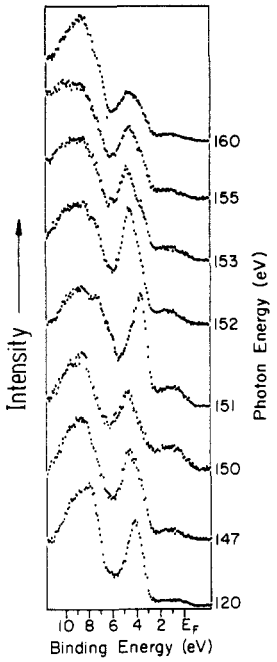

Figure 5. Photoemission spectra of six-monolayer equivalents of dysprosium on a 20-monolayer-thick film of FCC iron (grown on Cu(100). Spectra were taken across the 4d–4f giant resonance. Note the binding energy shift of the ^{7}F features (about 4 eV binding energy) at the incident photon energy of 151 eV. The light incidence angle was 60° off normal and all photoelectrons were collected normal to the surface.

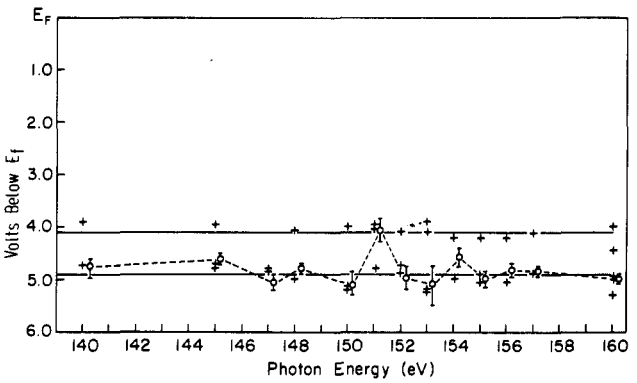

Figure 6. The binding energies of the two pronounced ^{7}F features as a function of photon energy (+). Note that unlike the combined feature binding energy (○), the individual features have binding energies independent of photon energy. The results are independent of substrate.

^{6}P, ^{6}D feature a resonance can be readily observed at the $5p_{1/2}$ threshold, while this resonance is weak and difficult to observe for the 5d band and the $^8S_{7/2}^{u+s}$ multiplet as seen in figure 3.

We find that the lower binding energy feature of 2.2 eV increases in intensity relative to the 3.1 eV binding energy feature with decreasing terbium film thickness for photon energies below 60 eV. In general there is also a shift in binding energy for these features

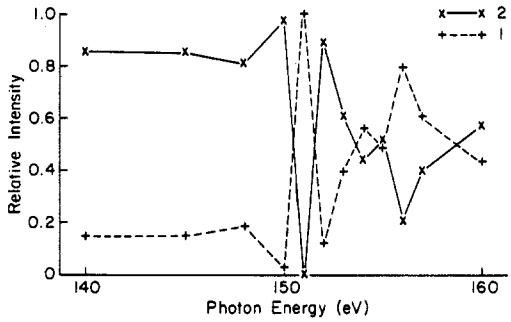

Figure 7. The relative intensities of the two ^7F features as a function of photon energy. The low binding energy feature is denoted by (---+---) while the higher binding energy feature is denoted by (—×—).

to smaller binding energies as seen in figure 4, while the other features shift to slightly greater binding energies as the film thickness decreases.

Figure 5 shows the energy distribution curves (EDCs) for the dysprosium valence band region for photon energies between 140 and 160 eV for dysprosium thin films on iron. As with terbium, the wealth of dysprosium 4f features can be identified by comparison with x-ray photoemission spectra [16–18]. The various multiplets are the $^7F_5$ and $^7F_6$ levels (at 4.1 ± 0.1 and 5.0 ± 0.1 eV), ^5L and ^5G levels (at 7.9 ± 0.2 eV), ^5I and ^5H levels (at 9.0 ± 0.2 eV), and the ^5K level (10.1 ± 0.2 eV).

As can be seen in figure 5, the ^7F feature binding energy is strongly dependent upon photon energy. By treating the ^7F multiplets as a combination of two features, analysis shows that the two contributing bands have binding energies independent of photon energy as seen in figure 6. For the two contributing features to the ^7F levels this has been plotted as a function of photon energy in figure 7. As seen in figure 7, the ^7F features show a very large shift in intensity from the high binding energy component to the low binding energy component at the 4d threshold. As with terbium, we observe that the relative 4f multiplet intensities vary with photon energy.

4. Discussion

We would now like to show that the 4f levels, even the resulting 4f multiplets, cannot be completely understood if correlation and interaction effects with other valence electrons are ignored, and that these effects are dependent upon the wave function symmetries. This is particularly true at or near a photoemission resonance.

4.1. Relative 4f multiplet cross-sections and final state effects

At the simplest level, studying a complete shell for example, multiplet splittings can be seen as an exchange polarization interaction between the spin of the unpaired valence electron and core level spins. Core level electrons with spins parallel to the valence electron spin will have a different binding energy than for antiparallel alignment by the amount of the exchange splitting [20]. When studying partially filled core levels, such as the rare earth 4f levels, a more complicated theory is required [7, 21]. In the central field approximation to an atom (neglecting spin interactions) there is an energy degeneracy in the m_l and m_s values. Since there are $g = 2(2l + 1)$ states of different m_l and m_s values in a shell nl, there is a degeneracy of

$$\binom{g}{N} = \left(\frac{g!}{(g-N)!N!}\right)$$

for N electrons in the shell. For two incomplete shells, the degeneracy becomes

$$\binom{g}{N}\binom{g'}{N'}.$$

The lifting of these degeneracies beyond the Hartree–Fock approximation is accomplished with perturbation theory.

Estimates of the numerous 4f multiplet intensities have been undertaken by Cox [7, 18] using a fractional parentage scheme that allows one to still use Slater determinants. This scheme does not provide any indication of photon energy dependence as we observe for terbium and dysprosium (figure 2) in the relative 4f intensities. Even off resonance this fractional parentage scheme does not agree with the experimental data. For example, the $^8S^u_{7/2}{}^s$ feature contains more than twice the intensity (37%) predicted by the fractional parentage scheme (14%) [7], if the 5d contributions are ignored.

In order to understand a major contribution to the deviations in the expected 4f multiplet intensities, it is important to look at the resonant photoemission process. Neglecting any lifting of degeneracies as a result of band symmetries, crystal field effects, and spin interactions there are a number of many electron excitations that can result in final states that contribute to the photoemission valence band spectra as seen in photoemission (as seen in table 1). In general the strongest photoemission resonances are the super Coster–Kronig transitions involving orbitals of the same principal quantum number [22–27], and for terbium these are:

$$4d^{10}5s^25p^64f^85d^16s^2 \rightarrow 4d^{10}5s^25p^54f^85d^26s^2 \rightarrow 4d^{10}5s^25p^64f^75d^16s^2$$

and

$$4d^{10}5s^25p^64f^85d^16s^2 \rightarrow 4d^95s^25p^64f^95d^16s^2 \rightarrow 4d^{10}5s^25p^64f^75d^16s^2$$

which with the super Coster–Kronig decay and emission from the 4f levels can share identical final states with direct emission from the 4f levels. The super Coster–Kronig transitions have been observed for many of the rare earth metals [23] and the references in [4] and are the major contributions to the 4f photoemission resonances observed for terbium and dysprosium as seen in figure 3 for terbium. Auger decay process with final states not identical with the direct photoemission processes can occur as outlined in table 1 [2] and could contribute some intensity to the 4f photoemission features at selected photon energies. For the most part, this additional complication will be ignored, but cannot be eliminated from contributing to our CIS spectra.

It has been observed that for the rare earth metals, the different unoccupied 5d and 4f symmetry states have different binding energies [4, 17, 18, 23, 24]. Because of these binding energy differences for the various 5d and 4f unoccupied states, a number of intermediate 'exciton' states will occur at slightly different photon energies. Thus the excitations outlined in table 1 do not account for any lifting of degeneracies as a result of symmetry. Such lifting of degeneracies as a result of different symmetries is also accompanied by alterations in the resonant photoemission threshold energy as has been conclusively demonstrated for gadolinium [4, 23]. These different core excited resonant photoemission processes differ principally in the symmetry of the wave function state of the core excited electron. For example, in the 5p to 5d resonant excitation, the core excitation could go as:

Table 1. Resonant photoemission processes for the valence bands for terbium.

Initial state	Excited state	Final state	Resonant threshold (eV)
$4d^{10}5s^25p^64f^85d^16s^2$	$4d^{10}5s^25p^54f^85d^26s^2$	$4d^{10}5s^25p^64f^85d^06s^2$	22 and 28
		$4d^{10}5s^25p^64f^85d^15s^1$	22 and 28
		$4d^{10}5s^25p^64f^85d^26s^0$	22 and 28
		$4d^{10}5s^25p^64f^75d^16s^2$	22 and 28
		$4d^{10}5s^25p^64f^75d^26s^1$	22 and 28
	$4d^{10}5s^15p^64f^85d^16s^26p^1$	$4d^{10}5s^25p^64f^85d^06s^2$	46
		$4d^{10}5s^25p^64f^85d^06s^16p^1$	46
		$4d^{10}5s^25p^64f^85d^16s^1$	46
		$4d^{10}5s^25p^64f^85d^16s^06p^1$	46
		$4d^{10}5s^25p^64f^75d^16s^2$	46
		$4d^{10}5s^25p^64f^75d^16s^16p^1$	46
		$4d^{10}5s^25p^64f^75d^06s^26p^1$	46
	$4d^95s^25p^64f^95d^16s^2$	$4d^{10}5s^25p^64f^85d^06s^2$	152
		$4d^{10}5s^25p^64f^85d^16s^1$	152
		$4d^{10}5s^25p^64f^95d^06s^1$	152
		$4d^{10}5s^25p^64f^95d^16s^0$	152
		$4d^{10}5s^25p^64f^75d^16s^2$	152
	$4d^95s^25p^64f^86d^16s^26p^1$	$4d^{10}5s^26p^64f^85d^06s^2$	151
		$4d^{10}5s^26p^64f^85d^06s^16p^1$	151
		$4d^{10}5s^26p^64f^85d^16s^1$	151
		$4d^{10}5s^26p^64f^85d^16s^06p^1$	151
		$4d^{10}5s^26p^64f^75d^16s^2$	151
		$4d^{10}5s^26p^64f^75d^16s^16p^1$	151
		$4d^{10}5s^26p^64f^75d^06s^26p^1$	151

$$p_x + ip_y\,(Y_1^1) \rightarrow d_{xz} + id_{yz}\,(Y_2^1)$$

$$p_z\,(Y_1^0) \rightarrow d_{3z^2-r^2}\,(Y_2^0)$$

or

$$p_x - ip_y\,(y_1^{-1}) \rightarrow d_{xz} - id_{yz}\,(Y_2^{-1})$$

ignoring spin–orbit coupling and the exchange splitting. The different core-excited 5d electron states clearly have different wave function overlap integrals and interactions with the different symmetry 4f states [27]. Thus excitations to different 5d or 4f symmetries will result in decay and emission of a 4f electron with a preferential symmetry [4] (as a result of Fermi's golden rule). This enhances one multiplet feature intensity over others. Because of the non-degenerate binding energies of the different symmetry 5d and 4f states, excitations to different 5d or 4f symmetries occurs at different photon energies. This is consistent with the different 4f partial cross-sections (figure 3) and relative 4f intensities (figure 2) observed for the different multiplet states of terbium and dysprosium.

The different widths of the resonant photoemission process for different initial state features must consider that different numbers of multiplet states contribute to the 'initial state' used in the CIS spectra. Several multiplet states contribute to the 'initial state' feature with a very broad photoemission resonance at the terbium 4d to 4f giant resonance, while only a narrow resonance is observed when only one multiplet state (the

terbium $^8S^{u,s}_{7/2}$) contributes to the 'initial state' feature as seen in figure 3. Nonetheless, because of the different symmetry considerations for the intermediate excited states, the appropriate joint density of states for the intermediate state may differ, resulting in different resonant photoemission widths.

4.2. Evidence for different screening channels

Cox and others predict that the $^8S_{7/2}$ 4f multiplet feature of terbium to be essentially only a singlet feature [7, 16–18, 28]. The photon energy dependence of this feature can only be understood if this feature is treated as the doublet indicated by the valence band photoemission (figure 1). If the $^8S^{u,s}_{7/2}$ multiplet feature is not split simply as a result of multiplet splittings intrinsic to the 4f levels then this doublet feature can only reasonably arise from three possibilities: a surface to bulk core level shift [29, 30], coexistence of multiple valencies ($4f^8 5d^1 6s^2$ or $4f^9 5d^0 6s^2$) [14, 15] or configuration interactions with the 5d electrons [7–13].

While the splitting of the terbium $^8S_{7/2}$ feature (approximately 1.0 ± 0.1 eV at 2–4 monolayers, 0.5 eV for thicknesses greater than 8 monolayers and 1 eV for bulk single-crystal terbium [31]) is only somewhat larger than the expected surface–bulk core level shift for the heavy rare earth metals of about 0.5 eV [29, 30], the photon energy dependence of these two features is difficult to reconcile with the surface to bulk core level shift. With increasing photon energy one expects the surface (higher binding energy) feature to decrease relative to the bulk feature (lower binding energy) feature because of the increasing photoelectron mean free paths. The relative intensities should also vary slowly with photon energy. As seen in figure 2, this behaviour is not observed. Indeed, as seen in figure 2, the resonance behaviour of the higher binding energy feature is not followed by similar behaviour in the lower binding energy feature. Such an observation is not expected for a surface to bulk core level shift doublet.

It is also possible to eliminate a surface to bulk core level shift as the source of the $^8S^{u,s}_{7/2}$ doublet on the basis of the terbium coverage dependent behaviour. For the heavy rare earths, the surface component has a greater binding energy than the bulk component [19, 29, 30]. For thinner rare earth films the surface contribution is large relative to the bulk contribution. For a surface to bulk core level shift, the $^8S^{u,s}_{7/2}$ feature should shift to the overall feature to a greater binding energy. This is not observed. These results cast some doubt upon the surface to bulk core level shift assignments for terbium and gadolinium [29, 30] made on the basis of selected photon energy dependent photoemission spectra and not coverage dependence [30].

There are strong thermodynamic arguments [14] that terbium, like gadolinium, is of only single valency and the surface does not have a different valence state from the bulk metal. Were there two different valencies for terbium, the other valency would have a 4f multiplet structure akin to dysprosium. This is not observed.

One of the most important simplifications to multiplet theory is the lack of configurational interactions [7]. Given that there are unpaired 5d electrons, known to be polarized [31], this assumption is very serious. Two different screening channels have been observed for the early rare earth metals, separating the 4f features by as much as 2.5 eV [12, 13, 32, 33]. Basically, the 4f hole can be screened by the 5d electrons near E_F, resulting in a 'fully screened' final state photohole. Alternatively, the 5d conduction band remains unpolarized (at room temperature both terbium and dysprosium are paramagnetic), and only weakly hybridizes with the 4f hole, thus providing only a poorly screened hole in the final state [12, 13]. This 5d to 4f hybridization, resulting in the

two different screening channels [12, 13], is very structure sensitive for cerium [34]. Additional complications may also occur including 'Fermi sea' correlation effects [6], and initial state 5d–4f hybridization, though the latter is not likely to be very pronounced. It is also important to realize that surface to bulk core level shifts can also not be completely eliminated from contributing to the 4f multiplet line shapes.

Changes in the 5d occupancy, as part of the excitation process will, of necessity, also change the Coulomb interaction, U_{fd}, between the 4f levels and the conduction band. With a super Coster–Kronig photoemission resonance as additional electron is placed into the conduction band. This changes the relative intensities between the screened ($^8S^s_{7/2}$ at lower binding energy for terbium) and unscreened ($^8S^u_{7/2}$ at higher binding energy for terbium) peaks $I_s/(I_s + I_u)$ at the photoemission resonance. This variation in the relative probability for decay through either screening channel near a photoemission resonance has been clearly observed with weakly bound adsorbates such as N_2 on Ni(100) [35]. We have plotted this variation in the screened versus unscreened channels in figure 2 for terbium.

While there exists a $^7F_5$ and $^7F_6$ doublet for dysprosium, accepting that the doublet is closely spaced, the above arguments can be applied to dysprosium as well as to terbium. Such a model can explain the 4f binding energy shifts (figure 6) and relative cross sections (figure 7) for dysprosium in much the same manner as has been applied to terbium. The complications of the multiplet doublet, and a surface to bulk core level shift are far harder to eliminate in the case of dysprosium than is the case for terbium.

The smaller energy difference between the screened and unscreened 4f states, as observed for terbium (1.0 eV) and dysprosium (0.6 eV), may be reconciled a weaker 4f–5d hybridization in the final state. Since the 4f levels are separated from the 5d conduction band by a far greater binding energy for terbium and dysprosium than is the case for cerium [17], a difference in the orbital overlaps leading to weaker hybridization in the case of Tb and Dy is reasonable. A shift of the $^8S_{7/2}$ features to smaller binding energies with decreasing coverage, as seen in figure 4, can now be understood as resulting from increased screening by d electrons of the 4f hole. The additional d electron density, leading to increased screening, can be donated by the nickel substrate, which has a high d band density of states near the Fermi energy.

The ratio of screened to unscreened decay probabilities has been shown by Riseborough [13] to be related to the ratio of the 5d–4f interaction, U_{fd}, and to the conduction band width, W. We observe two different screening channels for terbium, and possibly dysprosium as well, and in the model of Riseborough this implies that $(2l + 1)U_{fd} > W/2$ [13]. At or near a photoemission resonance $I_s/(I_s + I_u)$ cannot be evaluated in terms of the model of Riseborough [13]. Off resonance, using the model of Riseborough, $(2l + 1)U_{fd}/W$ is approximately equal to 0.53 ± 0.01 for terbium on nickel. Because of the complications of the ^7F multiplet structure, dysprosium cannot be reliably evaluated. Indeed, it may not be possible to apply the model and Hamiltonian proposed by Riseborough accurately to terbium and dysprosium. Nonetheless, a correlation between the 5d band and the 4f levels in the final state resulting in 4f satellite features in photoemission does suggest that other highly correlated states may exist in the final state, possibly resulting in satellite features for the 5d band, particularly at a super Coster–Kronig photoemission resonance where the interaction energy U_{fd} is seen to be large.

5. Conclusions

Analysis of resonant photoemission processes must consider the symmetry of the electron orbitals since the energy at which the resonance occurs is symmetry dependent, as

seen elsewhere [4, 23, 24] and can be inferred from the results of this work. Because decay routes are symmetry dependent, in the condensed state, partial cross-sections of the various final state photoemission features will also depend upon symmetry. It is abundantly clear that the different 4f multiplets do not and can not share identical cross sections in photoemission.

There is also evidence supporting two different screening channels in the photoemission from the 4f levels of terbium and dysprosium as well as cerium. This suggests that there is some final state hybridization of the 4f and 5d levels. Using the criterion of Riseborough, this implies that the Coulombic interaction energy between the 4f and 5d levels U_{fd} can only vary according to:

$$0.5 \leqslant (2l + 1)U_{fd}/W \leqslant 1.0$$

away from a photoemission resonance. This implies that the interaction energy is appreciable.

The results near resonance suggest that the core hole can indeed be very important as indicated by earlier work [8, 36, 37] and a single electron model is inappropriate for the 4f rare earth metals. Photoabsorption studies of terbium [38] also suggest that strong 4f to 5d hybridization, consistent with this work, but find little core hole perturbation of the adsorption spectra.

Acknowledgments

The authors would like to thank C G Olson for several fruitful discussions and Dan Wallace and the staff of the Synchrotron Radiation Center without whom this work would not have been possible. This work was supported by the US Department of Energy. The Synchrotron Radiation Center is supported by the NSF.

References

[1] Johansson L I, Allen J W, Lindau I, Hecht M H and Hagstrom S B M 1980 *Phys. Rev.* B **21** 1408
[2] Gerken F, Barth J and Kunz C 1981 *Phys. Rev. Lett.* **47** 993
[3] Lenth W, Lutz F, Barth J, Kalkoffen G and Kunz C 1978 *Phys. Rev. Lett.* **41** 1185
[4] Dowben P A, LaGraffe D and Onellion M 1989 *J. Phys.: Condens. Matter* **1** 6751
[5] Starace A F 1972 *Phys. Rev.* B **5** 1773
Dehmer J L and Starace A F 1972 *Phys. Rev.* B **5** 1792
[6] LaGraffe D, Dowben P A, Dottl L, Ufukteppe Y and Onellion M 1990 *Z Phys.* at press
[7] Cox P A 1974 *Structure and Bonding (Springer Tracts in Physics 24)* (Berlin: Springer) p 59
[8] Bagus P S, Freeman A J and Sasaki F 1973 *Phys. Rev. Lett.* **30** 850
[9] Liu S H and Ho K M 1982 *Phys. Rev.* B **25** 7052
[10] Liu S H and Ho K M 1983 *Phys. Rev.* B **28** 4220
[11] Norman M R, Koelling D D and Freeman A J. 1985 *Phys. Rev.* B **31** 625
[12] Riseborough P S 1985 *Physica* **130B** 66
[13] Riseborough P S 1986 *Solid State Commun.* **57** 721
[14] Johansson B 1979 *Phys. Rev.* B **19** 6615
[15] de Boer F R, Dijkman W H, Mattens W C M and Miedema A R 1979 *J. Less-Common Met.* **64** 241
[16] Baer Y and Busch G 1974 *J. Electron. Spectrosc. Relat. Phenom.* **5** 611
[17] Lang J K, Baer Y and Cox P A 1981 *J. Phys. F: Met. Phys.* **11** 121
[18] Cox P A, Lang J K and Baer Y 1981 *J. Phys. F: Met. Phys.* **11** 113
[19] LaGraffe D, Dowben P A and Onellion M 1989 *Phys. Rev.* B **40** 3348
[20] Freeman A J and Watson R E 1968 *Magnetism* vol IIA, ed G T Rado and H Suhl (New York: Academic) p 167

[21] Bethe H and Jachiw R 1964 *Intermediate Quantum Mechanics* (Menlo Park, GA: Benajamin–Cummings) p 120–48
[22] Zangwil A 1987 *Giant Resonances in Atoms, Molecules and Solids* ed X Connerade *et al* (New York: Plenum) p 321
[23] Baer Y and Scheider W D 1989 *Physics and Chemistry of Rare Earths* vol 10, ed K A Gschneider, L Eyring and S Hufner (Amsterdam: North-Holland) ch 10
[24] Lynch D and Weaver J H 1989 *Physics and Chemistry of Rare Earths* vol 10, ed K A Gschneider, L Eyring and S Hufner (Amsterdam: North-Holland) ch 4
[25] Allen J W, Johansson L I, Bauer R S, Lindau I and Hangstrom S B M 1978 *Phys. Rev. Lett.* **41** 1499
[26] Lenth W, Lutz F, Barth J, Kalkoffen G and Kunz C 1978 *Phys. Rev. Lett.* **41** 1185
[27] Egelhoff W F Jr, Tibbetts G G, Hecht M H and Lindau I 1981 *Phys. Rev. Lett.* **46** 1071
[28] McFeely F R, Kowaczyk S P, Ley L and Shirley D A 1973 *Phys. Lett.* **45A** 227
[29] Kammerer R, Barth J, Gerken F F, Flodsstrom A and Johannson L I 1982 *Solid State Commun.* **41** 435
[30] Gerken F, Barth J, Kammerer R, Johansson L I and Flodstrom A 1982 *Surf. Sci.* **117** 468
[31] Wu S C, Li H, Tian D, Quinn J, Li Y S, Jona F, Sokolov J and Christensen N E 1990 *Phys. Rev.* B **41** 11911 and references therein
[32] Parks R D, Raaen S, den Boer M L, Chang Y S and Williams G P 1984 *Phys. Rev. Lett.* **52** 2176
[33] Wieliczka D M, Olson C G and Lynch D W 1984 *Phys. Rev. Lett.* **52** 2180
[34] Wieliczka D, Weaver J H, Lynch D W and Olson C G 1982 *Phys. Rev.* B **26** 7056
[35] Dowben P A, Sakisaka Y and Rhodin T N 1984 *Surf. Sci.* **147** 89 and references therein
[36] Stern E A and Rehr JJ 1983 *Phys. Rev.* B **27** 3351
[37] Qi Boyon, Perez I, Ansari P H, Lu F and Croft M 1987 *Phys. Rev.* B **36** 2972
[38] Schutz G, Knulle M, Wienke R, Wilhelm W, Wagner W, Kienle P and Frahm R 1988 *Z. Phys.* B **73** 67